Energy & Environmental Science

Accepted Manuscript

ROYAL SOCIETY OF CHEMISTRY

www.rsc.org/ees

Journal Name

ARTICLE

Layered Phosphorus-Like GeP_5: a Promising Anode Candidate with High Initial Coulombic Efficiency and Large Capacity for Lithium Ion Batteries

Received 00th January 20xx,
Accepted 00th January 20xx

DOI: 10.1039/x0xx00000x

www.rsc.org/

Wenwu Li,[a] Huiqiao Li,*[a] Zhijuan Lu,[a] Lin Gan,[a] Linbo Ke,[a] Tianyou Zhai*[a] and Haoshen Zhou[b]

In this work, we for the first time investigate GeP_5 as an anode material for lithium ion batteries (LIB). By a facile high energy mechanical ball milling (HEMM) method, we successfully synthesize pure GeP_5 and GeP_5/C nanocomposite at ambient temperature and pressure. According to XRD Rietveld refinement and first principle calculation, GeP_5 holds an two-dimensional layered structure similar to black P and graphite, a high conductivity as 10000 and 10 times of black P and graphite, respectively. Serving as novel anode materials, both GeP_5 and its carbon composite deliver an unprecedented high reversible capacity of ca. 2300 mA h g^{-1}, combined with a high initial coulombic efficiency of ca. 95%. *Ex-situ* XRD and CV tests demonstrate GeP_5 undergoes conversion and alloying type lithium storage mechanism that its capacity is co-contributed by both Ge and P components. In addition, GeP_5/C exhibits superior cycle stability and excellent high-rate performance with a capacity of 2127 mA h g^{-1} at 5 A g^{-1}, suggesting their promising application in next-generation high-energy and high-power LIB.

Introduction

Graphite has dominated the anode materials in commercial lithium ion batteries (LIB) due to its high reversibility and low potential. However, the specific capacity of graphite is limited to 372 mA h g^{-1} corresponding to Li_xC_6 (x≤1). Moreover, graphite accommodates Li^+ at a low potential very close to that of Li plating, easily resulting in the safety problem of short circuit due to the formation of Li dendrite.[1-2] Therefore, many efforts have been devoted to exploring alternatives for graphite, with the hope of achieving simultaneously large capacities and proper potential to Li^+ intercalation.[3-6] Being the elements in same main group as carbon, silicon and germanium have been widely investigated as typical large capacity anode materials since they can store 4.4 unit Li per formula by forming $Li_{4.4}Si$ and $Li_{4.4}Ge$ alloys, corresponding to theoretical capacities of 4200 mA h g^{-1} and 1600 mA h g^{-1}, respectively.[7-11] However, both of them suffers from quite a large irreversible capacity loss (usually 20~50%) during the initial discharge/charge cycle due to their irreversible phase transitions and side reactions with electrolyte. Such a low coulombic efficiency at the first cycle dramatically limits the practical application of Si and Ge as anodes in full LIB. Moreover, their discharge/charge processes usually undergo huge volume expansion/contraction during the formation/decomposition of $Li_{4.4}M$ (M = Si, Ge) phases, which would severely degrade their cycle performances.

Apart from Si and Ge, elemental P, a low-cost abundant material locating in the fifth group of the periodic table, has attracted much attention in recent years for its high theoretical capacity of 2596 mA h g^{-1} according to the formation of Li_3P.[12-21] As known, there are three main allotropes for element P, including white P, red P and black P. White P begins to burn at 34 °C.[12] Red P suffers a very low coulombic efficiency (< 5%) at the first cycle.[12-14] In contrast, black P especially its carbon composites, are found able to demonstrate a large capacity of ~2000 mA h g^{-1} with good cycle stability.[12-13, 15] The much superior performance of black P than red P can be attributed to its graphite-like layered structure, which promises high electrical conductivity. Unfortunately, it is extremely difficult to fabricate black P because of the necessity of both high temperature and high pressure.[12-13] Worse, black P would be turned to red P at temperature above 125 °C.[12] As alternatives to black P, several metal phosphides (MP, M = transition metal), like MnP_4,[22-23] FeP,[24-26] CoP,[27] Ni_2P,[28-30] Cu_3P,[31] et al[32-34] have been explored, which show attractive lithium storage properties via a conversion reaction as $xLi^+ + xe^- + MP = Li_xP + M$, (M = Mn, Fe, Co, Ni, Cu *et al*).[1] Since these metals are inert for Li storage, the theoretical reversible capacities of these metal phosphides were usually less than 1200 mA h g^{-1}, much lower than that of black P. Besides, the reported metal phosphides usually show a very low first coulombic efficiency (<60%) and their cycle performances are

[a] *State Key Laboratory of Material Processing and Die & Mould Technology, School of Materials Science and Engineering, Huazhong University of Science and Technology (HUST), Wuhan 430074, Hubei, P. R. China*
E-mail: hqli@hust.edu.cn, zhaity@hust.edu.cn
[b] *Energy Technology Research Institute, National Institute of Advanced Industrial Science and Technology (AIST), Umezono 1-1-1, Tsukuba 305-8568, Japan*

Electronic Supplementary Information (ESI) available: [details of any supplementary information available should be included here]. See DOI: 10.1039/x0xx00000x

still poor. Therefore, it is of great interest to explore new P-based compounds which is easy-obtained and more stable than black P, but can provide a high specific capacity as elemental P.

In this work, we for the first time investigated a metal phosphide GeP_5 as the anode material for LIB. It can be easily obtained in a large scale by simply mechanical milling of elemental Ge and low cost red P. According to XRD refinement and structural analysis, GeP_5 holds a layered structure similar to black P and graphite, which promises the bonding feasibility with graphitic layer. Meanwhile, its conductivity is 10000 times higher than black P, and similar to that of graphite. Such high conductivity is considered very favourable for the lithium ion storage reaction. When served as an anode material, GeP_5 delivers a large specific capacity of 2266 mA h g^{-1}, much higher than those of metal phosphides mentioned above, due to its both reactive components of Ge and P for Li storage. Moreover, it can exhibit a first coulombic efficiency of 95%, to the best of our knowledge, which is the highest value among the reported anode materials up to now. By further compositing GeP_5 with conductive carbon in nanoscale, the cycle and rate performances of GeP_5 can be notably improved, which may profit from the homogeneous distribution of the active Ge and P components in the electrode, the good buffering to volume expansion by carbon matrix, and the existence of P-C bonds. In brief, as an anode material for LIB, GeP_5 exhibits excellent energy-storage properties comparable or surpass current reported results.

Results and discussion

Material synthesis, characterization and structural analysis

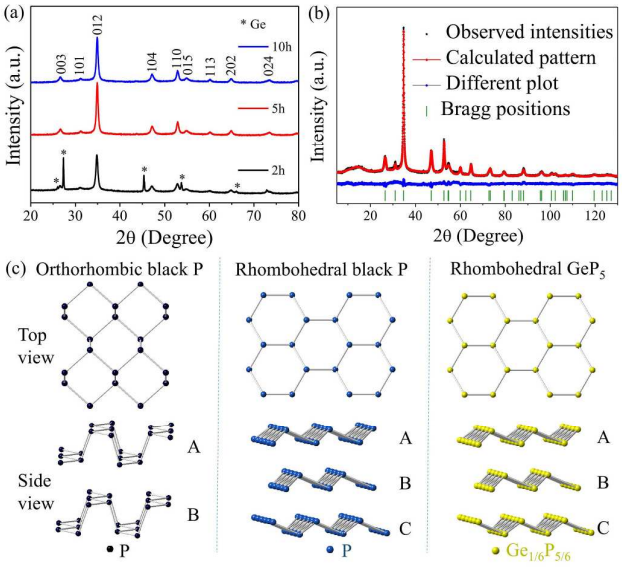

Figure 1. a) XRD patterns of as-synthesized powder products obtained at different ball milling time. b) Powder XRD patterns for Rietveld structure analysis of GeP_5. c) Crystal structure of orthorhombic black P, rhombohedral black P and rhombohedral GeP_5.

We fabricated GeP_5 with pure Ge powder and amorphous red P via high energy mechanical milling (HEMM). Simply, the mixture of Ge powder and red P, in a mole ratio of 1 to 5, was poured into HEMM vessel and after a certain milling time treatment, the GeP_5 powder can be collected in a large scale. The as-prepared GeP_5 is a crystalline powder. XRD tests in **Figure 1a** show that the diffraction peaks of GeP_5 phase can be clearly detected after 2 h ball milling, in spite of some residues of Ge peaks. Further, after 5 h milling, the peaks of Ge completely disappeared and all the observed peaks can be readily indexed to a pure GeP_5 phase (JCPDS Card No. 24-0455). Prolonging milling time to 10 h, the XRD pattern changes little but the intensity slightly decreased, suggesting degradation in GeP_5 crystal size or crystallization. As seen in SEM (**Figure 3a, 3b**) and TEM (Figure S1a) images, the GeP_5 sample obtained by 10 h milling is composed of large number of nanosized spherical particles which agglomerate into larger microsized secondary particles. HRTEM (in Figure S1b) on a typical GeP_5 particle shows its high crystalline nature, as ordered periodical lattice fringes with a d-spacing of 0.257 nm can be well observed, which evidences a crystalline GeP_5 particle with its (012) plane exposed to environment. The corresponding FFT pattern (Figure S1c) further confirms the single-crystalline nature of the particle.

XRD Rietveld refinement of GeP_5 was performed by using TOPAS. As shown in **Figure 1b**, all diffraction peaks can be well indexed by a rhombohedral cell in *R*-3*m* space group. Details of processing and refinement for GeP_5 including cell parameters, fractional atomic coordinates, and isotropic displacement parameters are given in Table S1-S2. The obtained parameters are highly close to the rhombohedral black P structure in which the unit cell contains six atoms in one identical atom site.[35-37] Since the XRD pattern of GeP_5 doesn't show any ordered occupation of Ge and P, the atom site is randomly occupied by Ge and P in a fixed occupation of p=1/6 and p=5/6, respectively (Figure S2). The crystal structural relationship between GeP_5 and black P are shown by **Figure 1c,** in which the GeP_5 structure can be taken as a derivate of rhombohedral black P except for different atoms. Rhombohedral black P has been reported a transition form of orthorhombic black P under high pressure above 50K bars,[35] the former holds a zigzag puckered structure while the latter holds an armchair ridge. In general, all of the three structures are of some similarities to that of graphite, e.g., a honeycomb-like lattice from the top view and a two-dimensional layered structure from the side view, although their puckered layers differ from the planar layer of graphite. Such a two dimensional layered structure is thought favorable to promise both high electrical conductivity and good structural flexibility for bonding with carbon. As reported, the electrical conductivity of GeP_5 is 1.0×10^6 S m^{-1},[37] which is nearly 10000 and 10 times higher than that of black P and graphite,[12] respectively (**Table 1**). The superior conductivity of GeP_5 to black P is consistent with the structural simulation results by first-principal calculations using density functional theory.[38-39] As shown in Figure S3, the density of states (DOS) for GeP_5 at the Fermi level is much larger than that of orthorhombic black

P, implying its much higher conductivity than black P. In addition, all the three structures of GeP_5, rhombohedral black P and orthorhombic black P show non-zero DOS at their Fermi levels, indicating they are all of metallic conductivities. Other calculated results including electron density difference (Figure S4), bonding information (Table S3), and related discussion are given in Supporting Information. With the layered structural features and high conductivity, GeP_5 is expected to be a promising anode material for LIBs.

Table 1. Comparison of graphite, black P and GeP_5 in theoretical capacity, density, and conductivity.[12,37]

Material	T_{cap} [mA h g^{-1}]	Density [g cm^{-3}]	Electrical conductivity [S m^{-1}]
Graphite	372	2.16	3.3×10^{2}~2×10^{5}
Black P	2596	2.69	0.2~3.3×10^{2}
GeP_5	2289	3.61	1.0×10^{6}

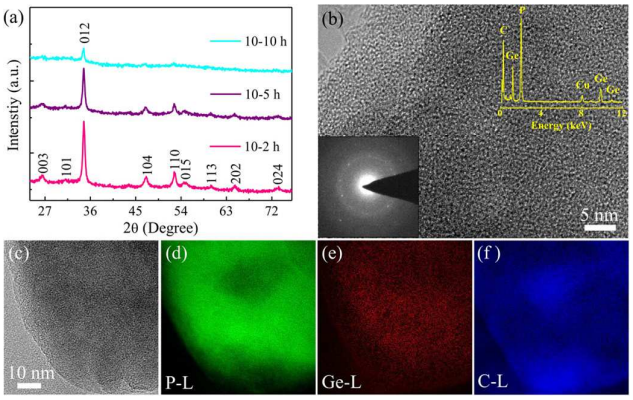

Figure 2. a) XRD patterns of GeP_5/C composite *versus* ball milling time. b) HRTEM, EDS (the inset at top right corner) and SAED (the inset at lower left corner) of GeP_5/C composite. c-f) Elemental mapping of GeP_5/C composite.

As we know, large capacity anode materials generally suffer poor cycle performance, therefore, combination them with carbon has been adopted widely to improve their cyclability.[40-41] For black P, Cui's groups[12] recently found that stable P-C bonds could be formed between P layers and graphitic layers in the composite of black P and carbon by high energy ball milling. And Wang's group[18] also found the chemical bonding phenomena between red P and graphene. The existence of P-C bonds endows the composite with high electrical conductivity, rapid charge-transfer processes and good lithium ion diffusivity for lithium uptake and extraction. Inspired by the structural similarity of GeP_5 to black P, here we prepared GeP_5/C composite via high energy ball milling of GeP_5 and Super P in a mass ratio of 7:2, expecting to combine this two layered materials by forming P-C like bonds at the interface of their layers to improve the electrochemical performances. **Figure 2a** gives the XRD patterns of GeP_5/C composite obtained at different ball milling time. After 5 h milling, the diffraction peaks can still be observed but with lower peak intensity and broader width. When increasing the milling time to 10 h, most of the diffraction peaks except for (012) have almost disappeared, suggesting a much lowered crystallnity of GeP_5 in the composite. **Figure 3c and 3d** show the SEM images of GeP_5/C obtained by 10-10 h milling. They show similar morphology and comparable particle size as that of pure GeP_5. The microstructure of GeP_5/C nanocomposite is observed by HRTEM. As shown in Figure 2b, the composite seems to be almost amorphous. Meanwhile, it can still find some ultrafine nanocrystals (< 5 nm) embedded into carbon matrix (Figure S5). These observations are in good agreement with the selected area electron diffraction image (SAED): a halo-like ring pattern with some dispersed spots. Energy-dispersive spectroscopy (EDS) indicates no impurity elements in the sample and the atom ratio of Ge and P is around 1 : 5. Elemental mapping analysis in **Figure 2c-2f** shows highly homogeneous distribution of elemental Ge, P and C in the GeP_5/C composite, indicating GeP_5 and C are effectively combined with each other to form an ultrafine nanocomposite during HEMM.

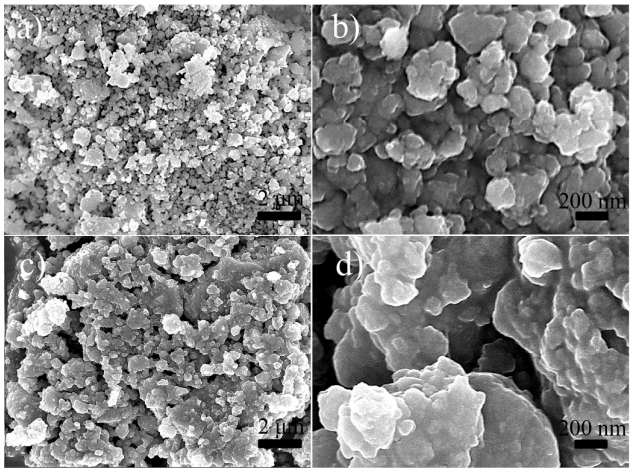

Figure 3. SEM images of a), b) pure phase GeP_5; and c), d) the 10-10 h milled GeP_5/C nanocomposites.

Lithium-storage performance

Figure 4a and 4c presents the discharge/charge profiles of GeP_5. At a current density of 200 mA g^{-1}, GeP_5 delivers a discharge and charge capacity of 2406 and 2266 mA h g^{-1} at the first cycle respectively, corresponding to a high initial coulombic efficiency of 95%. In contrast, pure black P was reported to exhibit only a reversible capacity of 1354 mA h g^{-1} with a much lower initial coulombic efficiency of 53.8%.[13] After 40 cycles, the capacity of pure GeP_5 gradually decreases to 250 mA h g^{-1}. And when the current density is increased from 0.1 A g^{-1} to 5 A g^{-1}, the rate capacity also decays fast from 2250 mA h g^{-1} to 200 mA h g^{-1}, as shown in Figure 4c. The dramatic capacity loss with cycle number and increased current densities suggests that pure GeP_5 undergoes large volume changes during Li^+ insertion/extraction processes. In comparison, the 10-10 h milled GeP_5/C nanocomposite (**Figure 4b and 4d**) shows much enhanced cycle stability and high-rate performance. The discharge/charge capacity of GeP_5/C

maintains almost constant at ca. 2300 mA h g^{-1} during 40 cycles with a coulombic efficiency approaching to 100%. At a current density of 1 A g^{-1}, the electrode can deliver over 1500 mA h g^{-1} after 150 cycles, as shown in Figure S6. Even at a high current density of 5 A g^{-1}, a specific capacity of 2127 mA h g^{-1} can still be obtained, which is more than fivefold the theoretical capacity of graphite (372 mA h g^{-1}). When the current is back to 0.1 A g^{-1}, the capacity recovers to 2361 mA h g^{-1} again. Besides, the 10-5 h milled GeP_5/C composite with medium crystallinity can also exhibit large capacity and superior cycle performance to pure GeP_5 (Figure S7).

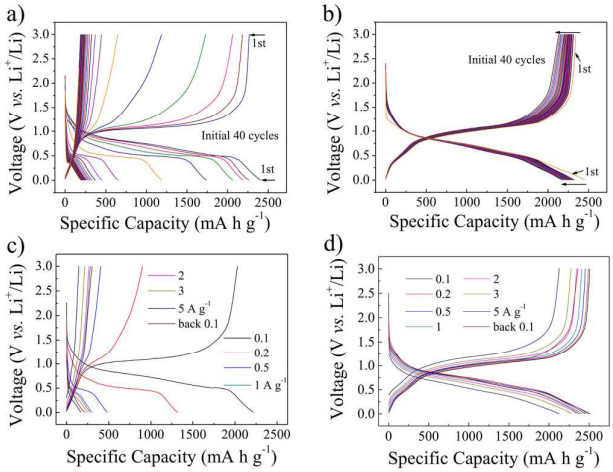

Figure 4. The discharge/charge profiles of a) Pure-phase GeP_5; b) GeP_5/C nanocomposite during the initial 40 cycles at a current rate of 0.2 A g^{-1}. The discharge/charge profiles of c) pure-phase GeP_5; d) GeP_5/C nanocomposite at different current rates between 0.005-3 V *vs.* Li^+/Li.

The much enhanced cycle stability and high rate performances of GeP_5/C nanocomposite are profited from the good combination and homogenously distribution of GeP_5 with carbon. According to Cui's and Wang's works,[12, 18] it is possible that P-C bonds are formed at the interface of GeP_5 layers and carbon layers during HEMM, due to the similarity of their structures. As shown in **Figure 5a**, compared with pure GeP_5, we can clearly see an extra broad Raman peak locating at 600~700 cm^{-1} in the GeP_5/C nanocomposite, which can be assigned to the P-C bonds between GeP_5 layers and graphitic layers of carbon.[12] In XPS spectra, an extra peak at 283.8 eV in the C 1s spectrum can be clearly found for GeP_5/C (**Figure 5b**). Besides, two extra peaks (**Figure 5c**) in GeP_5/C at 130.0 eV and 130.8 eV can also be found in the high-resolution spectra of P $2p_{3/2}$ and of P $2p_{1/2}$, respectively. The three extra peaks are thought also from the bonding between GeP_5 and carbon, since similar extra XPS peaks have been identified for the P-C bonds by Cui et al in the composite of black P and carbon.[12] As observed by TEM, ultrafine GeP_5 nanoparticles are highly dispersed in the continuous three dimensional conductive carbon networks. On the one hand, the carbon network provides directional electron-transport paths and tight electronic contact between the active nanoparticles, so that electrons can be quickly transferred from the active sites to the electrode current collector along the carbon superhighway. On the other hand, the volume expansion and consequential local strain generated upon Li^+ intercalation/extraction in active Ge and P components can be well buffered by flexible loose carbon matrix. Therefore, the GeP_5/C composite can well maintain the electrode integrity after cycling tests, as shown in **Figure 6a and 6b**. While for pure phase GeP_5 electrode (**Figure 6c and 6d**), both the top and cross-section view of its SEM images show that the active material is seriously peeling off from the current collector due to the electrode pulverizations after cyclic discharge/charge.

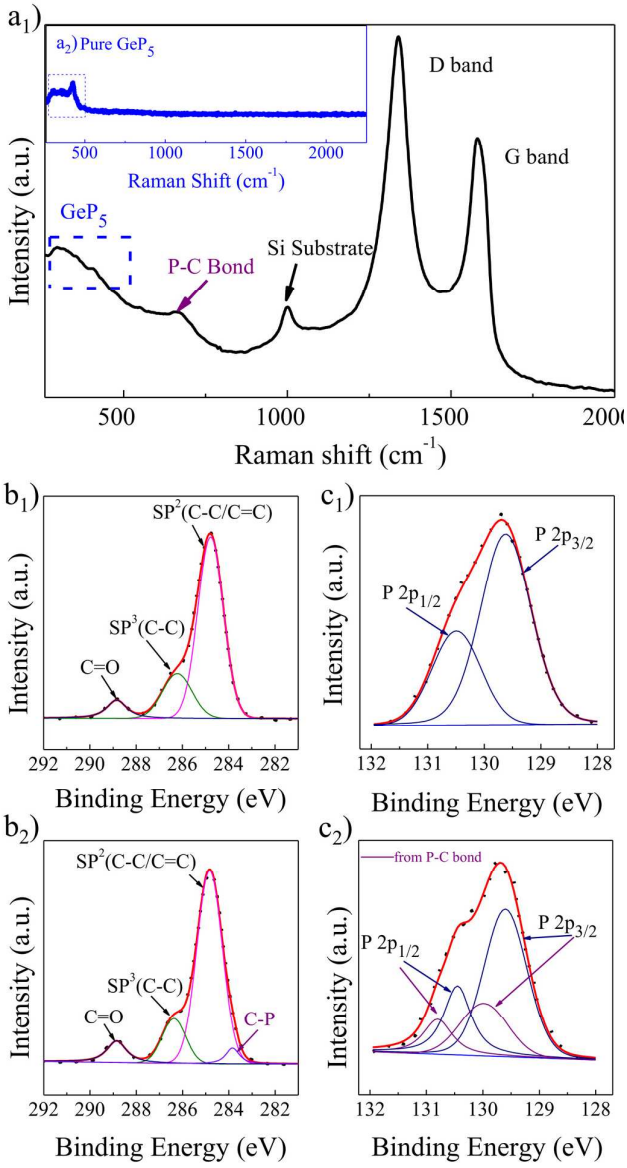

Figure 5. Raman spectra of GeP_5/C (a_1) and pure GeP_5 (the inset of a_1). XPS data of GeP_5 and GeP_5/C: the high-resolution C 1s spectra of GeP_5 (b_1) and GeP_5/C (b_2), respectively; the high-resolution P 2p spectra of GeP_5 (c_1) and GeP_5/C (c_2), respectively.

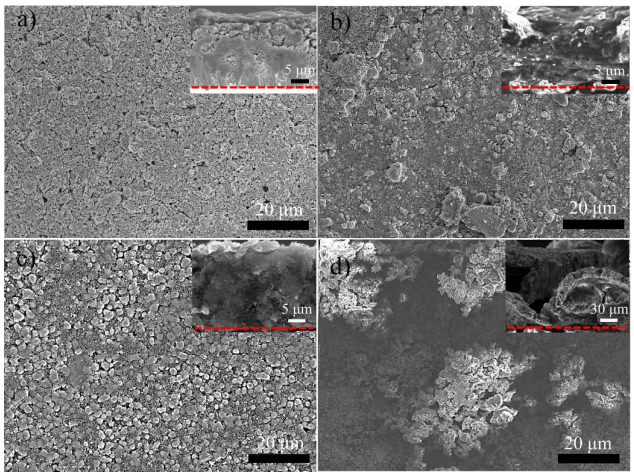

Figure 6. The SEM images of the GeP_5/C electrode: a) before cycling; b) after cycling. The SEM images of GeP_5 electrode: c) before cycling; d) after cycling. The corresponding cross-section images are given as the insets.

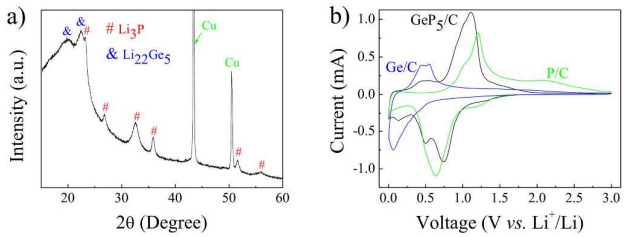

Figure 7. a) The *ex-situ* XRD pattern of GeP_5 electrode after the first discharge. b) The typical cyclic voltammetry curves of Ge/C, P/C and GeP_5/C electrode.

In order to investigate the lithium storage mechanism of GeP_5, we performed *ex-situ* XRD tests on the discharged electrode. As shown in **Figure 7a**, the GeP_5 electrode after discharging to 0.005 V clearly exhibits the XRD peaks of $Li_{22}Ge_5$ ($Li_{4.4}Ge$) and Li_3P phases,[27-28] which evidences the large capacity of GeP_5 comes from the contribution of both Ge and P. According to this, the electrode reaction of GeP_5 can be described by the following equations:

$$15\ Li^+ + 15\ e^- + GeP_5 \rightarrow Ge + 5\ Li_3P \quad (1)$$

$$4.4\ Li^+ + 4.4\ e^- + Ge \rightarrow Li_{4.4}Ge \quad (2)$$

$$\text{In total: } 19.4\ Li^+ + 19.4\ e^- + GeP_5 \rightarrow Li_{4.4}Ge + 5\ Li_3P \quad (3)$$

By **Equation 3**, the theoretical capacity of GeP_5 can be calculated to be 2289 mA h g^{-1} in which the five P atoms contribute 1770 mA h g^{-1} based on **Equation 1** and Ge atom donates the remaining capacity of 519 mA h g^{-1} based on **Equation 2**. As obtained by discharge/charge tests, the first charge capacity for GeP_5 is 2266 mA h g^{-1}, very close to the theoretical value, which indicates the completely reaction of GeP_5 for lithium storage as Equation 3. Besides, the density (Table 1) of GeP_5 is 1.67 and 1.34 times of graphite and black P,[12, 37] respectively, which would promise a much higher volumetric energy density in application.[34, 42] CV measurements on GeP_5/C in comparison of Ge/C and P/C composites further comfirm the above Li storage mechanism. As shown in **Figure 7b**, GeP_5/C sample exhibits two successive pronounceable peaks at 0.70~0.50V, followed by a small peak at 0.18 V during the negative scan. The peaks at 0.70~0.50V can well refer to the wide reduction peak of P/C sample at 0.65 V, which means this peak region is related to the conversion reaction between Li and GeP_5 to form Li_xP as denoted in Equation 1. While the peak at 0.18 V is observed well referred to the reduction peak of Ge/C sample at 0.1 V, which can be assigned to the further alloying of Li into Ge by forming Li_xGe as Equation 2. By comparing the peak symmetry as well as peak areas between cathodic and anodic scans, the two broad peaks observed at about 0.5 V and 1.1 V in positive scan can be assigned to the extraction of lithium from Li_xGe and Li_xP, respectively. These observations clearly show that GeP_5 undergoes synergistic Li-storage of both Ge and P. The potential differences between cathodic and anodic peaks in P/C and Ge/C are found larger than their counterparts in GeP_5/C, indicating the enhanced electrochemical kinetics of GeP_5 than elemental P and Ge. Figure S8 gives the CV curves of GeP_5/C at 1~30 cycles. During the initial two cycles, the reduction peak slightly shifts to higher potential and the oxidation peak becomes sharper, resulting in a smaller potential difference. This may be attributed to the decreased electrode polarization by initial activation of GeP_5/C in the first cycle of Li insertion/retraction. From the second cycle, the CV profiles show little changes in curve shape and peak area, confirming the high reversibility and good stability of GeP_5/C for Li storage.

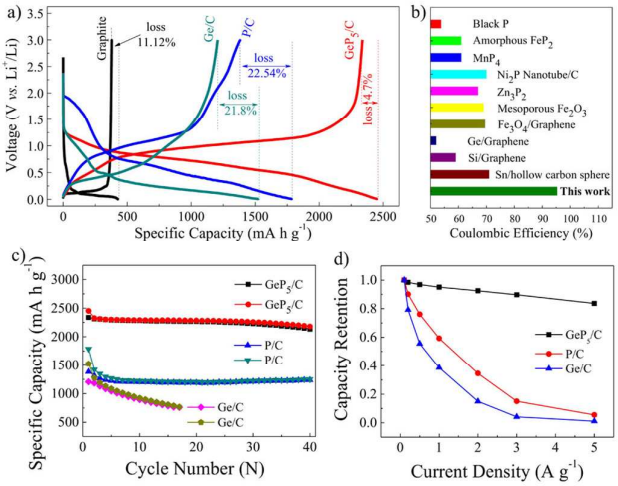

Figure 8. a) The first discharge/charge curves of GeP_5/C with graphite, Ge/C, and P/C anodes; b) comparison of initial coulombic efficiency of different anodes; c) cycling performances of GeP_5/C, Ge/C, and P/C at a current density of 0.2 A g^{-1}; d) rate capabilities of GeP_5/C, Ge/C, and P/C at current densities of 0.1, 0.2, 0.5, 1, 2, 5 A g^{-1}.

The coulombic efficiency especially at the first cycle of discharge/charge process is very important to an electrode material because it largely determines its practical application in a full battery. The bottle-neck of many large capacity anode materials for commercial utilization is their poor reversibility

between the first charge and discharge process. For GeP_5 and GeP_5/C, they can both show a very high first coulombic efficiency, which may ascribe to their excellent conductivity. As shown in Table 1, the conductivity of GeP_5 is $1.0x10^6$ S m^{-1}, nearly 10000 times and 10 times higher than black P and graphite, respectively. A similar case has been reported for RuO_2, who is also high conductive and can exibit a high first coulombic efficiency.[43] **Figure 8a** gives the first discharge/charge profiles of GeP_5/C in comparison of other anode materials. It can be seen that the capacity loss at the first cycle for P/C, Ge/C, nature graphite and GeP_5/C is 22.54%, 21.8%, 11.12% and 4.7%, respectively. Moreover, the obtained charge capacity of GeP_5/C is sixfold higher than graphite and 900 mA h g^{-1} higher than P/C anode. To ensure reasonable comparisons, we prepared Ge/C and P/C nanocomposites using HEMM method at the same experimental conditions as GeP_5/C. Detailed structure informations of the Ge/C and P/C samples are also obtained by SEM, EDS, XRD and TEM (Figure S9-S13). It can be noted that the particle size, shape, crystallinity and elemental distribution of Ge/C and P/C are comparable to those of GeP_5/C. In terms of the curve shape, GeP_5/C anode has non-stepped smooth discharge and charge plateaus and the voltage gap between discharge and charge plateaus is much narrower than those of P/C and Ge/C anodes. The smaller gap is very beneficial to get high energy efficiency and high-power performance when used in practical full batteries. Besides, GeP_5/C anode gives a relatively high lithium intercalation voltage, which is much safer than graphite and Ge/C anodes. These superior electrochemical behaviours of GeP_5/C to Ge/C and P/C may result from the synergetic effects of its high conductivity and bi-active components. The coulombic efficiency of GeP_5/C composite is observed as 95% at the first cycle and rapidly up to 100% from the second cycle, which reaches the level of commercial graphite. In contrast, many metal oxides, metal phosphides and alloy-type anodes like Si and Ge usually exhibit a first coulombic efficiency among 30~70%,[3-14, 16-17, 21-31, 40-41] much lower than that of commercial graphite (>85%), as illustrated in **Figure 8b**. The cycle performance and rate capability of GeP_5/C are presented in **Figure 8c** and **8d** in comparison with those of Ge/C and P/C. Both GeP_5/C and P/C show very stable cycle performances while the capacity of Ge/C decays fast with ascending cycle number. When increasing the current, the capacities of P/C and Ge/C decay very fast to less than 40% of their initial capacities while GeP_5/C can well maintain 85% of its initial capacity at the current increasing from 0.1 to 5 A g^{-1}. Referring to Cui's and Wang's works,[12, 18] P-C bonds are formed at the interface of GeP_5 layers and carbon layers during HEMM. The formation of P-C bonds would strengthen the structural resistance against the volume stress during Li^+ insertion/retraction, thus GeP_5/C and P/C can show much better cycle performances than Ge/C who cannot form P-C bonds. As for rate performances, the existence of P-C bonds together with the intermediate discharge/charge products of Ge and Li_xGe, would guarantee an excellent conductive network for the active P component. Thus, GeP_5/C can exhibit much higher rate performance than P/C and Ge/C.

Conclusion

In summary, we for the first time investigated the electrochemical performances of GeP_5 as an anode of LIB. Through a simple method of HEMM at ambient temperature and pressure, pure phase GeP_5 can be prepared in a large scale and high quality, from commercially available amorphous red P and Ge powders. The crystal structure is simulated by XRD Rietveld refinement and first principle calculation, respectively. GeP_5 exhibits a good reversible capacity of 2266 mA h g^{-1} with a first coulombic efficiency as high as 95%, much larger than those reported data for black P and other metal phosphides. The large capacity and high initial reversibility of GeP_5 are attributed to its high metallic conductivity and synergetic Li storage ability of its Ge and P components. Further, by forming an amorphous GeP_5/C nanocomposite, much enhanced rate performance and cycle stability can be achieved, e.g., a capacity of 2127 mA h g^{-1} at a high current of 5 A g^{-1} and a stable capacity of 2300 mA h g^{-1} after 40 cycles. The enhanced performance of GeP_5/C composite may result from the effective combination between GeP_5 and C layers which provides not only an integrated continuous conductive network but also a good structural flexibility to buffer the volume changes and resist the structure stress during Li^+ insertion/retraction. Briefly, integration of high first coulombic efficiency, large capacity, safe voltage, and excellent rate performance, GeP_5 and its carbon nanocomposite offer great promise as a high power and high energy anode for next-generation high performance LIB.

Experimental

Synthesis and Characterization of GeP_5 and GeP_5/C

Pure phase GeP_5 was synthesized by high energy mechanical milling (HEMM, Fritsch Pulverisette-6) of stoichiometric amounts of Ge (20 mmol) and amorphous red P (100 mmol) powder with a rotation speed of 400 rpm/min under Ar atmosphere. GeP_5/C nanocomposite was also obtained by HEMM the above-synthesized GeP_5 and Super P in a mass ratio of 7: 2 for 10 h at 400 rpm/min. For comparison, Ge/C and P/C samples were also prepared at the same condition in same weight ratio of Ge (or P): C = 7: 2. The synthesized products were characterized by a X-ray diffraction (XRD, PANalytical X'pert PRO-DY2198), a scanning electron microscope (SEM, FEI Sirion 200), a transmission electron microscope (TEM, FEI Tecnai G2 F30), a confocal Raman spectrometer (Raman, JobinYvon HR800) with a 532 nm excitation laser and a X-ray photoelectron spectrometer (XPS, AXIS-ULTRA DLD-600W) using an Al Kα.

Electrochemical Measurements

Electrochemical characterization was performed, using 2032 coin cells. The GeP_5/C anodes were prepared by pasting the paste containing 90 wt% of GeP_5/C and 10 wt% of Li-PAA onto a Cu foil. For comparison, the bare GeP_5 anode was made up of 70 wt% pure GeP_5, 20 wt% Super P and 10 wt% Li-PAA. The

loading of the active material is ca. 1.5-2 mg cm^{-2}. The electrolyte was 1.0 mol L^{-1} $LiPF_6$ dissolved in ethylene carbonate-diethyl carbonate (EC-DEC, 1:1 by vol.) solution. The lithium foil was performed as counter and reference electrodes. Cells were assembled in a glove-box with water-oxygen content below 1 ppm and tested at 25 ^{o}C. The galvanostatic discharge-charge tests were carried out on a LAND (Wuhan Kingnuo Electronic Co., China) cycler.

Acknowledgements

We acknowledge the support from National Nature Science Foundation of China (21571073, 51302099, 21322106), Ministry of Science and Technology of China (2015CB932600), Program for New Century Excellent Talents in University (NCET-13-0227) and National 1000 Young Talents Program of China. The authors are grateful to Prof. Zhiguo Xia, University of Science and Technology Beijing, for the structural simulation and Prof. Luying Li, Prof. Yihua Gao, and Dr. Jun Su from Wuhan National Laboratory for optoelectronics (HUST) for TEM tests and analysis. We thank the Analytical and Testing Center of Huazhong University of Science and Technology.

Notes and references

1 J. Cabana, L. Monconduit, D. Larcher and M. R. Palacín, *Adv. Mater.* 2010, **22**, E170-E192.
2 S. Y. Hong, Y. Kim, Y. Park, A. Choi, N. Choic and K. T. Lee, *Energy Environ. Sci.* 2013, **6**, 2067-2081.
3 M. S. Kishore and U. Varadaraju, *J. Power Sources* 2005, **144**, 204-207.
4 X. Xu, R. Cao, S. Jeong and J. Cho, *Nano Lett.* 2012, **12**, 4988-4991.
5 B. Wang, H. Wu, L. Zhang and X. W. (David) Lou, *Angew. Chem. Int. Ed.* 2013, **52**, 4165-4168.
6 W. Wei, S. B. Yang, H. X. Zhou, I. Lieberwirth, X. L. Feng and K. Mullen, *Adv. Mater.* 2013, **25**, 2909-2914.
7 C. K. Chan, H. Peng, G. Liu, K. Mcllwrath, X. F. Zhang, R. A. Huggins and Y. Cui, *Nat. Nanotechnol.* 2008, **3**, 31-35.
8 L. F. Cui, Y. Yang, C. Hsu and Y. Cui, *Nano Lett.* 2009, **9**, 3370-3374.
9 S. Chou, J. Wang, M. Choucair, H. Liu, J. A. Stride and S. Dou, *Electrochem. Commun.* 2010, **12**, 303-306.
10 S. Chou, Y. Zhao, J. Wang, Z. Chen, H. Liu and S. Dou, *J. Phys. Chem. C* 2010, **114**, 15862-15867.
11 K. T. Lee, Y. S. Jung and S. M. Oh, *J. Am. Chem. Soc.* 2003, **125**, 5652-5653.
12 J. Sun, G. Zheng, H. Lee, N. Liu, H. Wang, H. Yao, W. Yang and Y. Cui, *Nano Lett.* 2014, **14**, 4573-4580.
13 L. Sun, M. Li, K. Sun, S. Yu, R. Wang and H. Xie, *J. Phys. Chem. C* 2012, **116**, 14772-14779.
14 C. Park and H. Sohn, *Adv. Mater.* 2007, **19**, 2465-2468.
15 J. Qian, D. Qiao, X. Ai, Y. Cao and H. Yang, *Chem. Commun.* 2012, **48**, 8931-8933.
16 C. Marino, A. Debenedetti, B. Fraisse, F. Favier and L. Monconduit, *Electrochem. Commun.* 2011, **13**, 346-349.
17 L. Wang, X. He, J. Li, W. Sun, J. Gao, J. Guo and C. Jiang, *Angew. Chem. Int. Ed.* 2012, **51**, 9034-9037.
18 J. Song, Z. Yu, M. L. Gordin, S. Hu, R. Yi, D. Tang, T. Walter, M. Regula, D. Choi, X. Li, A. Manivannan and D. Wang, *Nano Lett.* 2014, **14**, 6329-6335.
19 J. Qian, X. Wu, Y. Cao, X. Ai and H. Yang, *Angew. Chem. Int. Ed.* 2013, **125**, 4731-4734.
20 J. Lee, J. H. Ryu, S. M. Oh and K. T. Lee, *Adv. Mater.* 2013, **25**, 3045-3049.
21 W. Li, S. Chou, J. Wang, H. Liu and S. Dou, *Nano Lett.* 2013, **13**, 5480-5484.
22 F. Gillot, L. Monconduit and M. L. Doublet, *Chem. Mater.* 2005, **17**, 5817-5823.
23 D. C. S. Souza, V. Pralong, A. J. Jacobson and L. Nazar, *Science*, 2002, **296**, 2012-2015.
24 S. Boyanov, J. Bernardi, F. Gillot, L. Dupont, M. Womes, J. M. Tarascon, L. Monconduit and M. L. Doublet, *Chem. Mater.* 2006, **18**, 3531-3538.
25 J. W. Hall, N. Membreno, J. Wu, H. Celio, R. A. Jones and K. J. Stevenson, *J. Am. Chem. Soc.* 2012, **134**, 5532-5535
26 W. Li, S. Chou, J. Wang, H. Liu and S. Dou, *Chem. Commun.* 2015, **51**, 3682-3685.
27 M. C. López, G. F. Ortiz and J. L. Tirado, *J. Electrochem. Soc.* 2012, **159**, A1253-A1261.
28 Y. Lu, J. Tu, Q. Xiong, J. Xiang, Y. Mai, J. Zhang, Y. Qiao, X. Wang, C. Gu and S. X. Mao, *Adv. Funct. Mater.* 2012, **22**, 3927-3935.
29 Y. Lu, J. Tu, Q. Xiong, Y. Qiao, J. Zhang, C. Gu, X. Wang and S. X. Mao, *Chem. Eur. J.* 2012, **18**, 6031-6038.
30 Y. Lu, J. Tu, C. Gu, X. Wang and S. X. Mao, *J. Mater. Chem.* 2011, **21**, 17988-17997.
31 M. S. Chandrasekar and S. Mitra, *Electrochim. Acta* 2013, **92**, 47-54.
32 J. Qian, Y. Xiong, Y. Cao, X. Ai and H. Yang, *Nano Lett.* 2014, **14**, 1865-1869.
33 W. Li, S. Chou, J. Wang, J. H. Kim, H. Liu and S. Dou, *Adv. Mater.* 2014, **26**, 4037-4042.
34 Y. Kim, Y. Kim, A. Choi, S. Woo, D. Mok, N. Choi, Y. S. Jung, J. H. Ryu, S. M. Oh and K. T. Lee. *Adv. Mater.* 2014, **26**, 4139-4144.
35 J. C. Jamieson, *Science* 1963, **139**, 1291-1292.
36 T. Kikegawa and H. Iwasaki, *Acta* Cryst. 1983, **B39**, 158-164.
37 P. C. Donohue and H. S. Young, *J. Solid State Chem.* 1970, **1**, 143-149.
38 D. Su, S. Dou and G. Wang, *Nano Energy* 2015, **12**, 88-95.
39 J. P. Perdew and Y. Wang, *Phys. Rev. B* 1992, **45**, 13244-13249.
40 X. Zhou, Y. Yin, L. Wan and Y. Guo, *Adv. Energy Mater.* 2012, **2**, 1086-1090.
41 D. Xue, S. Xin, Y. Yan, K. Jiang, Y. Yin, Y. Guo and L. Wan, *J. Am. Chem. Soc.* 2012, **134**, 2512-2515.
42 N. Yabuuchi, M. Kajiyama, J. Iwatate, H. Nishikawa, S. Hitomi, R. Okuyama, R. Usui, Y. Yamada and S. Komaba, *Nat. Mater.* 2012, **11**, 512.
43 P. Balaya, H. Li, L. Kienle and J. Maier, *Adv. Funct. Mater.* 2003, **8**, 621-625.

Layered Phosphorus-Like GeP_5: a Promising Anode Candidate with High Initial Coulombic Efficiency and Large Capacity for Lithium Ion Batteries

Wenwu Li,[a] Huiqiao Li,*[a] Zhijuan Lu,[a] Lin Gan,[a] Linbo Ke,[a] Tianyou Zhai*[a] and Haoshen Zhou[b]

Keywords: GeP_5, layered structure, phosphorus-like, anode, lithium ion batteries

Table of Content

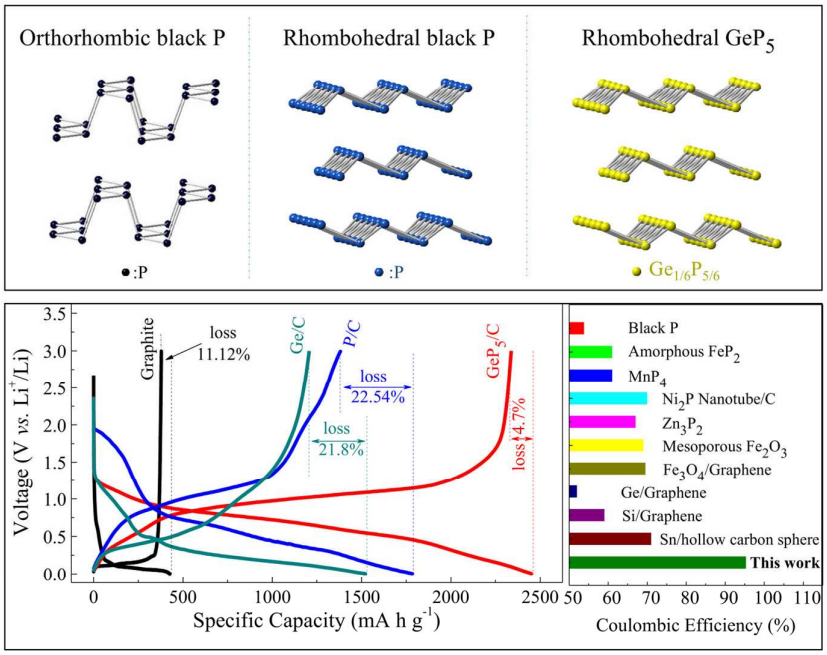

Layer structured GeP_5 is firstly developed as an anode material for LIB, it delivers a reversible capacity of 2300 mA h g^{-1} with a very high initial coulombic efficiency of 95%.

Broader context

Although great progresses had been made in last two decades, the performances of lithium-ion batteries are still far below the requirements of vehicle industry especially in comparison with the energy and power density of combustion engines. To make a breakthrough in energy and power density, new electrode materials must be searched to take place the current utilized $LiCoO_2$ cathode and graphite anode. For anode, various materials such as conversion-type metal oxides and alloy-type Si, Ge, Sn have been proposed as the alternatives of graphite. They are all capable to deliver a capacity several times that of graphite. However, none of them can behave a high reversibility as graphite. These large capacity materials usually suffer a very low initial coulombic efficiency (< 70%) and undergo a rapid capacity loss during cycling, which make them difficult to use in full batteries. Here, we for the first time develop GeP_5 as a new anode candidate. It holds a two-dimensional layered structure and a high electronic conductivity as graphite. It can deliver an unprecedented high capacity of ~2300 mA h g^{-1} with a high initial coulombic efficiency of 95%, which is the highest value in reported anodes to our best knowledge.